Noise Hunting:
Mitigating and Eliminating Noise Sources in Virgo

Nathan Flood
Pittsburg State University

July 31, 2017

Contents

Abstract

In this paper we'll analyze the methods and tools developed and used at Virgo prior to entering the 2017 observing run with aLIGO (O2). In addition we'll discuss the noise sources mitigated and/or eliminated. In this time period Virgo had the greatest single gain in sensitivity in Virgo history (+10Mpc in binary neutron star range). It is through the culmination of all these efforts that Advanced Virgo was able to achieve a new record sensitivity, paving the way for the first ever triple interferometer detection. These tools and methods used in this noise hunting campaign may also contribute to future noise hunting campaigns. If during O2 Virgo and aLigo have a triple detection this could provide not only an triangulated sky location, but with the sky location particle detectors may be able to better observe the particles emitted by the cosmic event detected. This would provide the opportunity to further understand these extraordinary cosmic events.

1 Introduction

Noise hunting is a critical role in the commissioning phase of the interferometer. After the reinstallation of steel suspensions the interferometer noise hunting was prioritized so as to join LIGO for the last part of O2 (observing run). Virgo joining O2 provides the opportunity for the first ever triple interferometer detection. With a triple detection we'll be able to better approximate sky location. With a better sky approximation we can then 'point' particle telescopes more precisely, which could provide further information about the observed cosmic event (e.g. black hole black hole merger).

In this paper we'll first introduce the tools used in the pre-O2 noise hunting phase, these include: *DataDisplay*, *BruCo*, correlation and spectrograms. In addition to the tools we'll also duscuss some of the methods and 'success' stories of the pre-O2 noise hunting campaign.

2 Noise Hunting Tools

2.1 *DataDisplay*

Within the *DataDisplay* interface there are many of the necessary tools for effective noise hunting. *DataDisplay* provides a user interface for generating analyzing data from all channels at Virgo. The tools in *DataDisplay* include, but are not limited too fast Fourier transforms (FFTs), coherence, spectrograms, and the change of coherence in time. Many initial observations of noise sources are made in *DataDisplay* then *MATLAB* or *Python* tools are used for any additional analysis needed.

The first and often simplest check for some noise source is to check the coherence. Coherence is mathematically defined as a function between two signals say $x(t)$ and $y(t)$ such that

$$\gamma^2_{xy}(f) = \frac{|S_{xy}(f)|^2}{S_{xx}(f)S_{yy}(f)}$$

where $S_{xy}(f)$ is the cross-spectral density functions of $x(t)$ and $y(t)$, respectively. While the underlying mathematics is important to understand for the sake of brevity the value of $\gamma^2_{xy}(f)$ is bound in the interval $0 \leq \gamma^2_{xy}(f) \leq 1$. If $\gamma^2_{xy}(f) = 1$ then it can be said these signals are linearly related or perfectly correlated, however if $\gamma^2_{xy}(f) = 0$ they are uncoherent or said to have zero coherence. It is important to note that any non-linear process that generates noise, such as scattered light, will

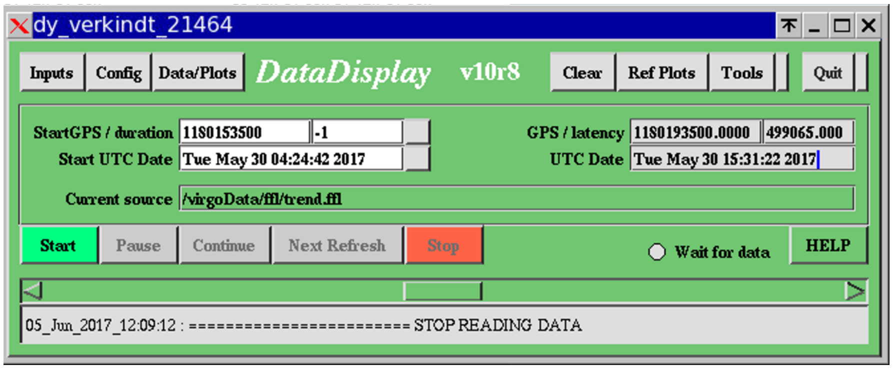

Figure 1: *DataDisplay* user interface

produce no coherence. It is also important to note that typically coherence seen in a 'flat' bands (no sharp lines) can usually be be disregarded. Coherence can be the first tool for a noise hunter and works well for noise sources such as acoustic or electromagnetic noise.

In addition to checking coherence *DataDisplay* is capable of generating plots in the time domain and frequency domain (FFTs). Looking at sensors in the time domain can be helpful for determining the change of say temperature or position with respect to time. Time domain data is also useful for determining when the interferometer is locked and the quality of the lock. It is important to note that dark fringe data (e.g. LSC_DARM, Hrec_hoft, etc.) are only useful when the interferometer is locked. To check not only whether the interferometer is locked, but also the quality of the lock one must generate a time domain plot of both the Hrec_Flag_Lock and Hrec_Range_BNS. The flag channel is simply a one if the interferometer is locked and zero otherwise. The Range channel gives a range of detection of a binary neutron star inspiral, currently a good lock has a BNS range of $\approx 24Mpc$. However, that depends on the current status of the interferometer. After checking for a quality lock one can use dark fringe data for analysis.

2.2 *BruCo*

BruCo is short for brute force correlation, and was written by Gabriele Vajente. Essentially *BruCo* takes some main channel (typically LSC_DARM) and looks at all channels in the Virgo database for coherence. The output of the coherence is written to the web in a large matrix.

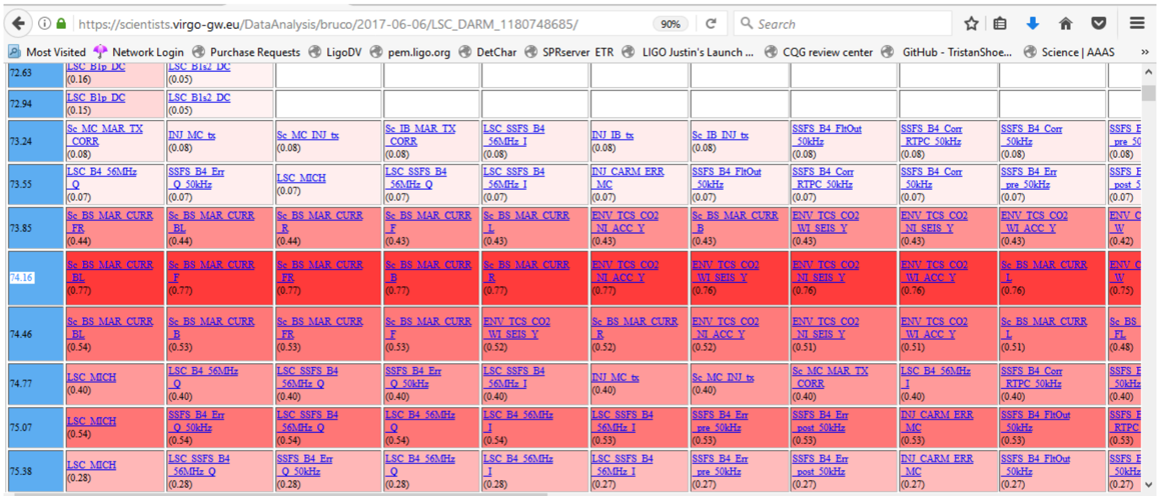

72.63	LSC B1p DC (0.16)	LSC B1s2 DC (0.05)									
72.94	LSC B1p DC (0.15)	LSC B1s2 DC (0.05)									
73.24	Sc MC MAR TX CORR (0.08)	INJ MC tx (0.08)	Sc MC INJ tx (0.08)	Sc IB MAR TX CORR (0.08)	LSC SSFS B4 56MHz I (0.08)	INJ IB tx (0.08)	Sc IB INJ tx (0.08)	SSFS B4 FltOut 50kHz (0.08)	SSFS B4 Corr RTPC 50kHz (0.08)	SSFS B4 Corr 50kHz (0.08)	SSFS E pre 50 (0.08)
73.55	LSC B4 56MHz Q (0.07)	SSFS B4 Err Q 50kHz (0.07)	LSC MICH (0.07)	LSC SSFS B4 56MHz Q (0.07)	LSC SSFS B4 56MHz I (0.07)	INJ CARM ERR MC (0.07)	SSFS B4 FltOut 50kHz (0.07)	SSFS B4 Corr RTPC 50kHz (0.07)	SSFS B4 Corr 50kHz (0.07)	SSFS B4 Err pre 50kHz (0.07)	SSFS E post 5 (0.07)
73.85	Sc BS MAR CURR FR (0.44)	Sc BS MAR CURR BL (0.44)	Sc BS MAR CURR R (0.44)	Sc BS MAR CURR F (0.43)	Sc BS MAR CURR L (0.43)	ENV TCS CO2 NI ACC Y (0.43)	Sc BS MAR CURR B (0.43)	ENV TCS CO2 WI SEIS Y (0.43)	ENV TCS CO2 NI SEIS Y (0.43)	ENV TCS CO2 WI ACC Y (0.43)	ENV C W (0.42)
74.16	Sc BS MAR CURR BL (0.77)	Sc BS MAR CURR F (0.77)	Sc BS MAR CURR FR (0.77)	Sc BS MAR CURR B (0.77)	Sc BS MAR CURR R (0.77)	ENV TCS CO2 NI ACC Y (0.77)	ENV TCS CO2 WI SEIS Y (0.76)	ENV TCS CO2 NI SEIS Y (0.76)	ENV TCS CO2 WI ACC Y (0.76)	Sc BS MAR CURR L (0.76)	ENV C W (0.75)
74.46	Sc BS MAR CURR BL (0.54)	Sc BS MAR CURR B (0.53)	Sc BS MAR CURR FR (0.53)	Sc BS MAR CURR F (0.53)	ENV TCS CO2 WI SEIS Y (0.52)	Sc BS MAR CURR R (0.52)	ENV TCS CO2 NI ACC Y (0.52)	ENV TCS CO2 NI SEIS Y (0.51)	ENV TCS CO2 WI ACC Y (0.51)	Sc BS MAR CURR L (0.51)	Sc BS FL (0.48)
74.77	LSC MICH (0.40)	LSC B4 56MHz Q (0.40)	LSC SSFS B4 56MHz Q (0.40)	SSFS B4 Err Q 50kHz (0.40)	LSC SSFS B4 56MHz I (0.40)	INJ MC tx (0.40)	Sc MC INJ tx (0.40)	Sc MC MAR TX CORR (0.40)	LSC B4 56MHz I (0.40)	SSFS B4 Corr RTPC 50kHz (0.40)	SSFS E 50kHz (0.40)
75.07	LSC MICH (0.54)	SSFS B4 Err Q 50kHz (0.54)	LSC SSFS B4 56MHz Q (0.54)	LSC B4 56MHz Q (0.54)	LSC B4 56MHz I (0.54)	LSC SSFS B4 56MHz I (0.53)	SSFS B4 Err pre 50kHz (0.53)	SSFS B4 Err post 50kHz (0.53)	INJ CARM ERR MC (0.53)	SSFS B4 FltOut 50kHz (0.53)	SSFS E RTPC (0.53)
75.38	LSC MICH (0.28)	LSC SSFS B4 56MHz Q (0.28)	SSFS B4 Err Q 50kHz (0.28)	LSC B4 56MHz Q (0.28)	LSC B4 56MHz I (0.28)	LSC SSFS B4 56MHz I (0.27)	SSFS B4 Err pre 50kHz (0.27)	SSFS B4 Err post 50kHz (0.27)	INJ CARM ERR MC (0.27)	SSFS B4 FltOut 50kHz (0.27)	SSFS E 50kHz (0.27)

Figure 2: Screenshot of *BruCo* output

Within the *BruCo* output matrix different channels are highlighted with differing shades of red. The first column of the output is the frequency in LSC_DARM that *BruCo* looked for coherence. The remaining columns are the most coherent channels at that given frequency, where the more red a cell is the more coherent that channel is. Because *BruCo* looks for coherence with *all channels* often it can return 'false positives.' In the words of Federico Paoletti, *"Too much information is no information at all."* From a noise hunting standpoint it is usually far more helpful to look at the ENV *BruCo*. Using the ENV configuration *BruCo* only looks for coherence with environmental sensors, which can make the output far easier to understand and much less saturated.

BruCo is one of the most useful tools available for finding noise sources that are coupled linearly. This is typically sharp narrow lines more so than wide structures. As per usual, generally all 50 Hz harmonics can be ignored. Again because coherence only looks for some linear coupling *BruCo* is not typically useful when it comes to non-linear processes, such as scattered light or non-stationary lines.

2.3 Correlation

While *DataDisplay* and *BruCo* are useful for stationary structures for non-stationary structures, in frequency or amplitude, a correlation can be run. This is particularly useful for drifting lines (see Section 3.4).

The method used for correlation is simply a linear regression. The program used for pre-O2 correlation was written by Soumen Koley. This *MATLAB* script is yet to be documented, but will eventually be published and documented. The program itself is fairly simple and straight forward, but is quite computationally intensive. In the input file the user must provide a GPS start time, GPS stop time, main channel to check for correlation (usu. LSC_DARM), and a few other minor inputs. The user also provides a list of lines to follow in time and check correlation (central frequency of line and bandwidth of line).

The script first obtains the main channel data throughout the entire GPS time specified, usually on the order of days, disregarding unlocked periods. While obtaining this data the the program is also following the progression of the input lines in time. Then, once the lines have been followed the program looks for correlated channels (i.e. channels that are moving in the same way). On the

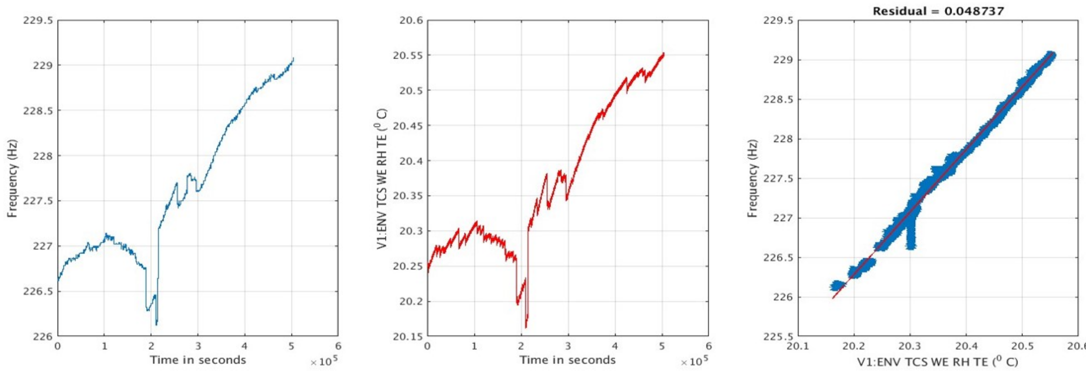

Figure 3: *Left:* Drift in Frequency, *Mid:* WE temperature Drift, *Right:* Fit Line

left of Figure 3 is the frequency of some line as it drifts in time, the middle is the channel that correlation was found, the temperature of the west end ring heater. This is correlation is achieved by applying a linear regression model, then calculating the residuals. Conceptually the residual is a measurement of the quality if the fit line. As you can see in Figure 3 on the right this correlation is very good in the sense that the points all lie very closely to the line fit. This linear regression is ran for all relevant channels, then the models are sorted by the residual calculated. For a more detailed mathematical description of the program see the documentation once the program is published.

2.4 Spectrogram

DataDisplay is capable of generating spectrograms, however these are very computationally intensive and can often crash *DataDisplay*. A spectrogram is a graphic representation of the evolution of the FFT in time. These are very useful for identifying the characteristics of a structure in time. Is it stable in frequency? Is it stable in amplitude? Is it always present? Spectrograms are particularly helpful if they are generated over a long time period. However these cannot be generated reliable in *DataDisplay* and must be generated using the root command. For instance Figures 8, **??**, **??**, and **??** were generated over a ten day period. Within the Virgo database spectrograms are calculated continuously for certain relevant channels. The root command pulls directly from this data, this prevents from having to constantly re-calculated the spectrograms.

3 Advanced Virgo pre-O2 Noise Hunting

Turbo pumps are used throughout Virgo as part of the vacuum system. There are turbo pumps located on all towers, in addition there are pumps throughout the different linkage tubes in the central building. Throughout the progression of Virgo, from Virgo to Virgo Plus to now Advanced Virgo turbo pumps have been often sources of noise. Depending on the situation if a line seen in the dark fringe is associated with a turbo pump it must be determined whether the turbo pump is vital to the operation of the interferometer. That being said the role of a noise hunter is to categorically identify the culprit of some noise, it is left to the team that 'owns' the noise source to determine a method of mitigation.

3.1 Turbo Pump

We first saw good coherence with the three lines in LSC_DARM centered at $456.5Hz$ and all the accelerometers in the central building.[1] Of the accelerometers the ENV_BS_ACC_Z seemed to have the best coherence suggesting the source was closest to the beam splitter. It was known that there are two turbo pumps near the beam splitter, one on the the beam splitter signal recycling link (*TP1*) and the other on the beam splitter power recycling link (*TP2*). In an attempt to distinguish the two pumps operational frequency we moved the signal recycling accelerometer to different positions.[2] During this test we moved the accelerometer closer to *TP1*, closer to *TP2* and various distances from both turbo pumps. The results of the test were very conclusive. As you can see in the logbook entry the $456.5Hz$ lines increased when close to *TP1*, decreased when close to *TP2* and the entire floor decreased when the accelerometer was far from everything, as expected. This implied that the *TP1* was responsible for the lines seen in LSC_DARM.

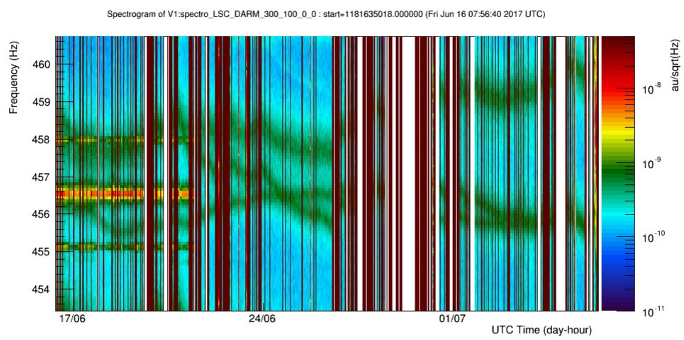

Figure 4: Spectrogram of LSC_DARM after *TP1* Switch OFF

It was decided by the VAC team that this pump was redundant and unnecessary for operation, thus it was switched off removing the lines from LSC_DARM.[3] It is worth noting that while this did improve the sensitivity curve there was not obvious improvement in range.

3.2 Mercury Motor Controller

The Mercury Motor Controller investigation was conducted in a similar fashion with respect to the turbo pump investigation. During some 'sniffing' around with a spectrum analyzer [4] it was observed that a small server rack (dubbed minirack) located to the left at the entrance of the central building was emitting electromagnetic lines similar to the comb of approximately 10 lines seen in LSC_DARM centered at $2496Hz$. We then investigated the lines more closely with a high resolution portable analyzer. Upon investigation the lines were strongest near the Mercury Motor Controllers (*Note: Mercury is the brand name of the MMCs*).In addition momentarily switch-

[1]elog #37927
[2]elog #38007
[3]elog #38176
[4]Federico Paoletti

ing off the MMCs eliminated the lines from the spectrum analyzer. We then installed a temporary magnetic probe into the Virgo database for monitoring the MMCs and checking coherence.

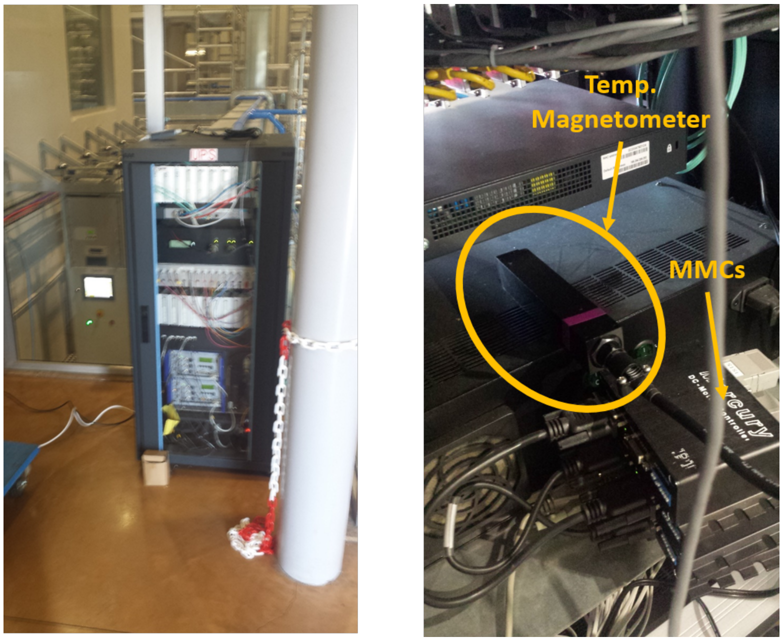

Figure 5: *Left:* Minirack *Right:* Mercury Motor Controllers and temporary magnetometer

Once dark fringe was achieved and the interferometer was locked good coherence was seen with all lines in the comb. The injection team was consulted to see whether these controllers could be switched off without serious consequences, and per their recommendation the MMCs were switched off removing the comb from LSC_DARM. It is worth noting the MMCs control the position of four lenses on the External Injection Bench (EIB1) and are rarely used. Again similar to the turbo pump investigation there was no noticeable gain in sensitivity, however this did remove a total of fourteen lines from LSC_DARM.

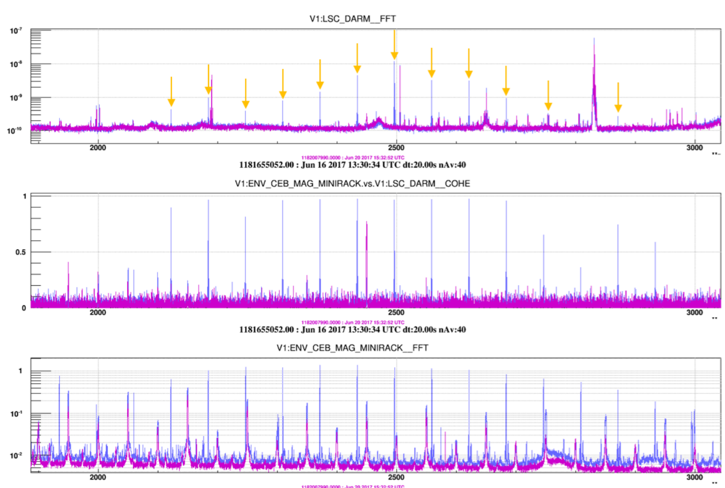

Figure 6: LSC_DARM and Magnetometer with MMCs on and off

3.3 Switch OFF Test

Both the Mercury Motor Controller and Turbo Pump noise elimination were localized to the Environmental Noise Team, however the mass switch OFF included almost every commissioning team and was a large scale effort to switch OFF all nonessential device near the interferometer. This included unneeded VAC equipment, ENV sensors, SUSP motor drivers, and several other smaller subsystems.[5] After the global switch OFF 50 Hz decreased by a factor of about twenty, this resulted in an increase of the Binary Neutron Star range of one megaparsec.

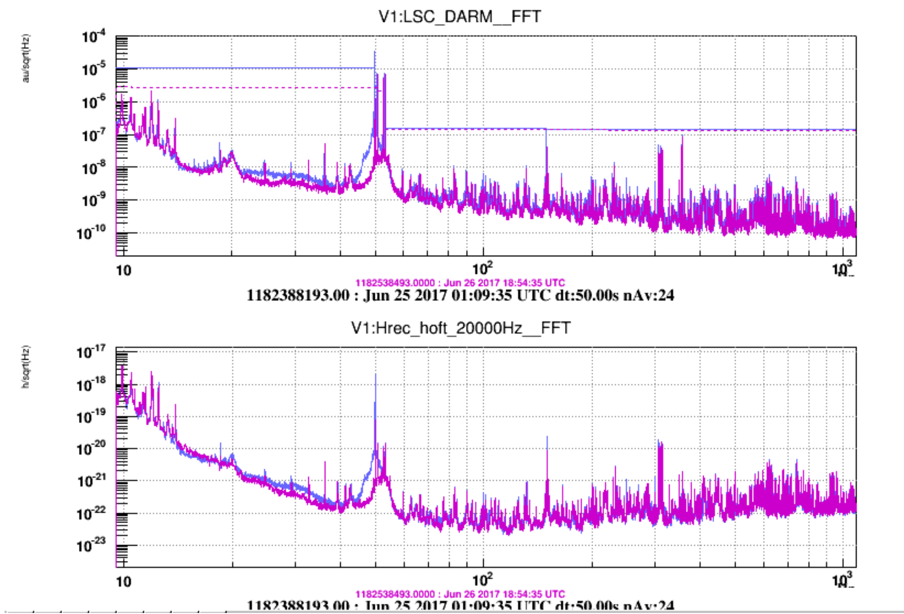

Figure 7: 50 Hz Before and After Switch OFF

While many of the items switched OFF were considered nonessential they can only be off temporarily. Thus a strategic switch ON was planned to determine which items were responsible for the decrease in the 50 Hz line. Initially the suspected source was an improperly isolated fan. So, with the interferometer locked the fan was switched back ON, there was no observable change in the 50 Hz line. In an attempt to optimize the switch ON process things were switched on in groups with the interferometer locked and the 50 Hz line was monitored. The 50 Hz amplitude seemed most dependent on the motor driver racks for the the west input and west end. Upon further investigation (individual selective switch on), it was determined the source of the excessive noise was the last stage motor drivers for the suspensions of the west end and input towers. In principle the north arm motor driver configuration should be identical to the west arm, however switching ON the last stage motor drivers for the north arm seemed to induce no additional noise. That being said these drivers were determined to be nonessential, thus switched off for both the north and west arms.[6]

[5] elog #38250, elog #38246
[6] elog #38399

3.4 Drifting Lines

It was first observed on June 18th [7] that there seemed to be some lines in the spectrum that drifted in frequency, some went up in frequency some went down. It was this post that spurred a further investigation. Initially these lines were identified using spectrograms over ten or more days. By inspection we were able to see there seemed to be some correlation with temperature in the central building and both end buildings.

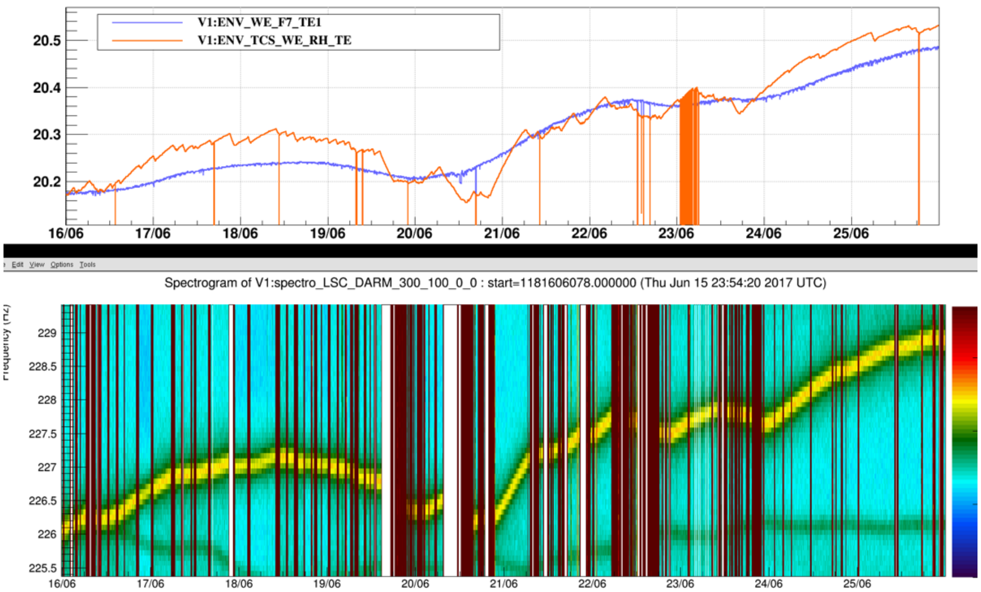

Figure 8: Initial correlation with temperature by inspection

It is well known that many noise sources can change frequency as temperature changes. However, it is very strange that these lines were correlated and anti-correlated (mirror images of temperature trend). It was well understood that because of the anti-correlated lines it could not be some simple mechanical mode that generated the lines. In addition the drift of frequency was on the order of hertz per tenth of a degree Celsius, far too large for a simple mechanical mode. It was proposed that maybe the anti-spring used in the suspensions was complex enough to be capable of generating anti-correlation, but there was very little evidence or method of testing this hypothesis.

3.4.1 Grouping of Families and Correlation

By inspection we were able to group the drifting lines into families. *See Figure 9.*

[7] elog #38079

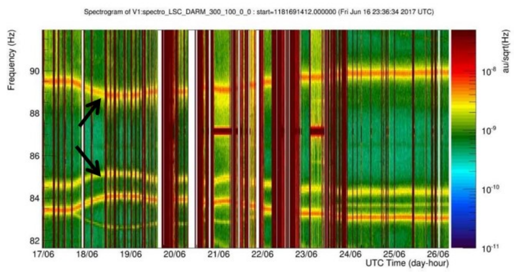

(a) Family 1

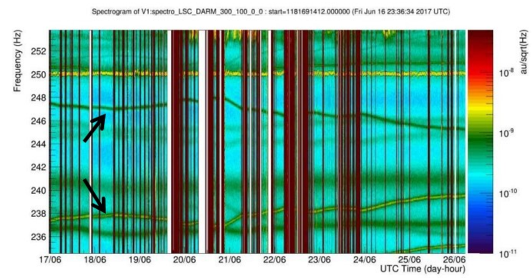

(b) Family 2

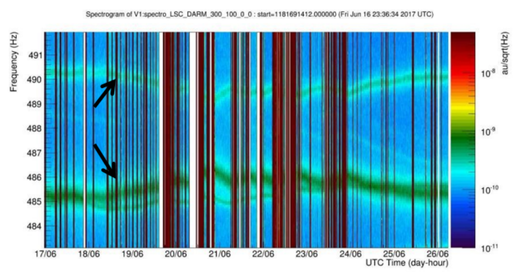

(c) Family 3

Figure 9: Families of Drifting Lines

Browsing a spectrogram of LSC_DARM up to $500Hz$ by hand we developed a list of over one hundred drifting lines divided into these three families. We then took the list of lines from each family and ran a correlation. The correlation results[8] showed dependence on the ring heater temperature sensors (directly above the mirrors) and the vertical position of the mirror (LVDT). The so called family 1 was dependent on the LVDT and temperature of the west input and north input(i.e. central building temperature). Family 2 was dependent on west end temperature and LVDT, and lastly family 3 was correlated to the temperature of the north end. Initially it was theorized that the drift may have been dependent on the vertical position of the mirror. Several tests were conducted.

3.4.2 Tests Conducted

The simplest and least invasive test proposed was to shake the suspension from the top. It was theorized that the crosswires responsible for positioning the mirror were soft, and shaking the the suspension would likely verify if the crosswires were the cause of the issue. The west input tower was shaken, however the lines associated with the west input did not drift.

The second test attempted was to change the vertical position of the mirror. We moved the west input mirror first down $170\mu m$ from its nominal position then up $110\mu m$ again from the nominal position. This movement was equivalent change in temperature on the order of tenths of degrees Celsius. Essentially if the drift was a function of vertical position, we would have expected a drift

[8]See Section 7.2 for top five correlated channels

of frequency on the order of several hertz. There was no drift of any lines observed. This ruled out the possibility of it being some defect on the mirror surface.

The last test conducted was to heat the mirror with the ring heaters(*Figure* **??**)[9] Prior to this test a high sampling frequency channel ($50kHz$) was added to monitor if there were drifting lines at high frequency. This was the first successful test tat resulted in a controlled drift of the lines.

Mirror Heating Test Results

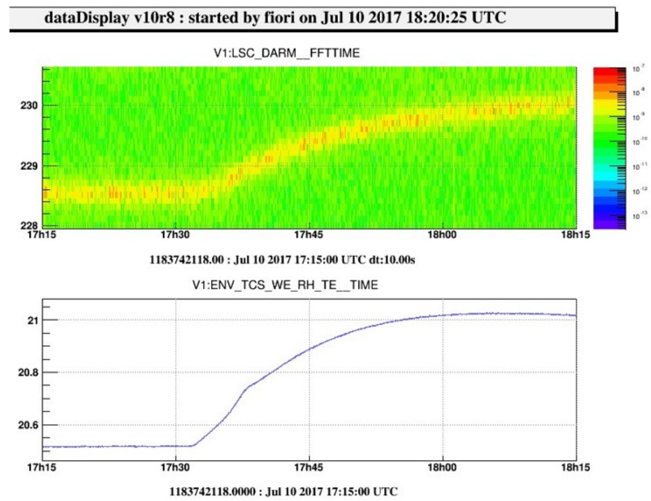

During this test it was also observed that the 'drum' modes of the mirrors also drifted. The 'drum' lines are higher order oscillatory modes of the mirrors. It is worth noting that it is fairly well known from models the frequency of the 'drum' modes, however the higher the order the mode of oscillation the more uncertainty there is in the model. Essentially this means that we know there are higher orders of oscillation, but we are unsure of their exact location on the spectrum. We observed that the drifting lines began to drift at exactly the same time the 'drum' mode lines began to drift.

3.4.3 Aliasing Filters

Through the combination of seeing the 'drum' modes drift with temperature and the presence of mirror images it was realized that this may be an issue of aliasing.[10] Aliasing is a well documented phenomenon in data acquisition. Again for the sake of brevity we'll assume the reader is familiar with aliasing filters, if not refer to the aliasing filter article sited in Section 6. Essentially the ADC sampling rate was set too high to where the present anti-aliasing filters were ineffective. With the butterworth AAS set at 80 KHz you would typically need a sampling rate of more than 600kHz to prevent aliasing. However, in the drifting lines scenario the ADC sampling rate was set at 100kHz, essentially these means the noise from 50kHz to 100kHz is folded back into the spectrum. It is believed that these so called drifting lines are some mirror mode around 100kHz being folded back into the spectrum.

The results of the improvement of the anti-aliasing filters were quite drastic. Overnight when the ADCs were updated LSC_DARM saw the disappearance of not only the drifting lines, but also a huge decrease in the overall noise floor. This resulted in the biggest single gain in BNS range in Virgo history from nine Mpc to nineteen Mpc.

[9] elog #38529
[10] elog#38533

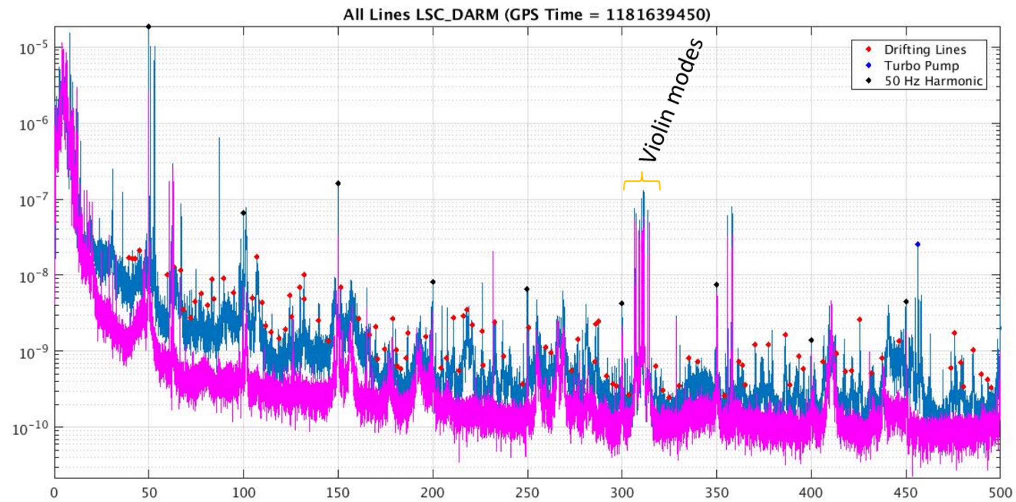

Figure 10: LSC_DARM Before and After Noise Hunting

4 Conclusion

The pre-O2 noise hunting has provided many useful tools and techniques for future noise hunting teams. One can argue that the largest contribution to the noise hunting tools is the Correlation tool written by Suomen Koley. This tool was responsible for correctly correlating all the drifting lines to the temperature in their respective towers. This ultimately lead to a ten megaparsec gain in BNS range. Throughout the history of Virgo, there has never been another time like this. In every instance that a noise source was identified it was decided that the source could either be switched OFF entirely or easily mitigated in some way. In previous noise hunting campaigns often several methods were attempted over the course of several days or weeks to mitigate the noise. Where as most noise in this campaign was mitigated within only a few days. The success of this campaign was partially due to the pressure to join O2 and a little bit of luck.

5 Acknowledgments

I want to thank my adviser and the leader of this noise hunting campaign Irene Fiori, for her constant willingness to help me no matter how busy she was. Also special thanks to Soumen Koley for knowing everything there is to know about *Matlab*, and for letting me bounce ideas off of you. Thanks you to Josẽ from the Pisa lab and Laura from the Nikhef group. Thanks to all the Frenchies Raphaël, Lèa, Benjàmin, Davìd and Matthièu, for your willingness to share a Tenet's and discuss physics. And of course thank you to the National Science Foundation and the University of Florida for funding and organizing this phenomenal opportunity.

6 Useful References and Further Reading

- Virgo Monitoring (VIM) Webpage (*BruCo*, long term spectrograms, current status of ITF, etc.): https://vim.virgo-gw.eu

- *BruCo* Documentation: https://dcc.ligo.org/DocDB/0118/G1500230/001/LVC_03_2015_BrucoNonStat.pdf

- root Documentation: https://root.cern.ch

- Magnetic Probe Documenation: https://scientists.virgo-gw.eu/EnvMon/List/FluxGateMagnetometer/fluxGateMagn_m

- Accelerometer Documetation: https://scientists.virgo-gw.eu/EnvMon/List/Accelrometers/393B12/393B12_H.pdf

- Mechanical Mode Shapes: https://tds.virgo-gw.eu/ql/?c=11995

7 Appendix

7.1 Advanced Virgo Diagram

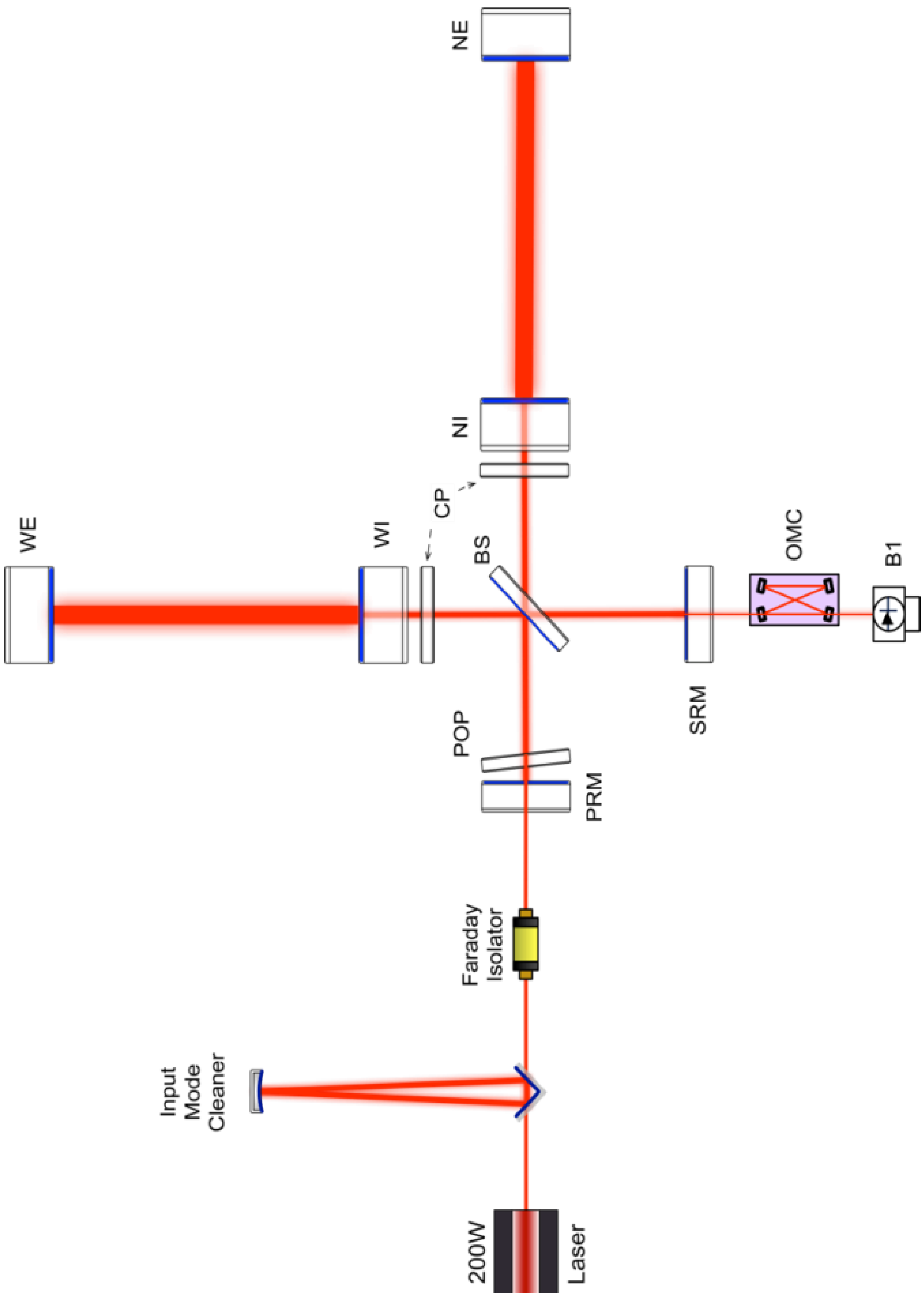

7.2 Correlation Results

Family 1 Correlation Results

	Top 5 Correlated Channel
1	V1:INF_TCS_NI_RH_TE
2	V1:INF_TCS_WI_RH_TE
3	V1:Sa_WI_F7_LVDT_V_mean
4	V1:ENV_WI_F7_TE2
5	V1:ENV_WI_F7_TE1

Family 2 Correlation Results

	Top 5 Correlated Channel
1	V1:ENV_TCS_WE_RH_TE
2	V1:ENV_WE_MIR_COIL_UL_TE
3	V1:ENV_WE_MAR_COIL_FL_TE
4	V1:SBE_SWEB_F0_y_mean
5	'V1:SBE_SWEB_LVDT_F0Vraw_mean

Family 3 Correlation Results

	Top 5 Correlated Channel
1	V1:ENV_TCS_NE_RH_TE
2	V1:ENV_NE_MIR_COIL_UL_TE
3	V1:SBE_SNEB_LVDT_F0Vraw_mean
4	V1:SBE_SNEB_F0_y_LVDT_10Hz_mean
5	V1:SBE_SNEB_F0_y_mean